

## Surface-Isomerization Dynamics of *trans*-Stilbene Molecules Adsorbed on Si(100)-2×1

Damien Riedel,<sup>\*,†</sup> Marion Cranney,<sup>†</sup> Marta Martin,<sup>†</sup> Romain Guillory,<sup>†</sup>  
Gérald Dujardin,<sup>†</sup> Mathieu Dubois,<sup>‡</sup> and Philippe Sonnet<sup>§</sup>

*Laboratoire de Photophysique Moléculaire, CNRS (UPR 3361), Bât. 210, Centre Universitaire de Paris Sud, F91405 ORSAY, France, MINATEC/INPG/IMEP, 3 Parvis Louis Néel, BP 257, F-38016 Grenoble Cedex 1, France, and Institut de Science des Matériaux de Mulhouse (IS2M) LRC CNRS 7228 - Université de Haute Alsace 7014 4, rue des Frères Lumière 68093 Mulhouse Cedex, France*

Received September 21, 2008; E-mail: damien.riedel@u-psud.fr

**Abstract:** Photoinduced *trans*–*cis* isomerization studies of stilbene molecules in the gas phase have led to a precise understanding of the corresponding molecular dynamics. Yet, when such molecules are adsorbed on surfaces, these reactions are expected to be strongly modified as compared to what is known in the gas phase. In this work, a low temperature (5 K) scanning tunneling microscope (STM) is used to image the *trans*-stilbene molecules deposited on a Si(100)-2×1 surface at 12 K. *trans*-Stilbene undergoes conformational changes during the adsorption process such that four different stilbene conformers are observed: *trans*-stilbene (TS), *cis*-stilbene (CS), and two new conformers I<sub>1</sub> and I<sub>2</sub>. Furthermore, electronic excitation of individual stilbene molecules, by means of tunnel electrons, is shown to activate specific reversible molecular surface isomerization (TS ↔ I<sub>1</sub> and CS ↔ I<sub>2</sub>) combined with diffusion across the surface. Calculated STM topographies, using the tight binding method, indicate that the CS and TS molecules are physisorbed. The molecular conformations of the surface isomers I<sub>1</sub> and I<sub>2</sub> are suggested to be analogous to transient state conformations of the stilbene molecule when stabilized by the silicon surface. The measurements of the molecular surface isomerization and diffusion reaction yields are used to build a qualitative potential energy surface of the various stilbene reactions. The molecular surface-isomerization dynamics is shown to be influenced by the type of dopant (n or p). This is related to surface charging, which reveals modifications in the stilbene ionization potential.

### 1. Introduction

Isomerization and especially *trans*–*cis* photoisomerization reactions of aromatic molecules have been extensively studied in the gas and liquid phases during the past few decades.<sup>1–5</sup> Stilbene molecules have been, in particular, thoroughly explored because they are considered as a model for *trans*–*cis* isomerization studies.<sup>6</sup> Furthermore, they are ideal candidates for molecular electronics due to their properties of organic conductors, photoswitches, organic displays, or biosensors.<sup>7–10</sup> Photoexcitation of stilbene in the gas phase shows a competition

between the *trans*–*cis* isomerization and the photocyclization mechanism forming dihydrophenanthrene.<sup>6</sup> The description of the *trans*–*cis* photoisomerization in the gas phase arises from the so-called one-bond flip (OBF) mechanism acting on the C–C double bond of the molecule.<sup>6,11</sup> When stilbene is confined in a limited volume such as in matrices, the number of degrees of freedom of the molecule is reduced, and the description of the isomerization is modified. The OBF mechanism is much less probable than the so-called hula-twist (HT) mechanism in which only one CH group of the double bond rotates out of plane.<sup>12</sup> However, recent work has shown that the HT mechanism can also take place in free stilbene molecules, leading to *cis*–*trans* isomerization.<sup>13</sup>

Isomerizations have been studied for molecules adsorbed on surfaces<sup>7,14–27</sup> by activating the reactions via photon excitation,<sup>21</sup> by means of tunnel electrons or with the electrostatic

<sup>†</sup> Centre Universitaire de Paris Sud.

<sup>‡</sup> MINATEC/INPG/IMEP.

<sup>§</sup> Université de Haute Alsace.

- (1) Rau, H.; Waldner, I. *Phys. Chem. Chem. Phys.* **2002**, *4*, 1776–1780.
- (2) Kucharski, S.; Janik, R.; Motschmann, H.; Radüge, Ch. *New J. Chem.* **1999**, *23*, 765–771.
- (3) Baskin, J. S.; Bañares, L.; Pedersen, S.; Zewail, A. H. *J. Phys. Chem.* **1996**, *100*, 11920–11933.
- (4) Leitner, D. M.; Levine, B.; Quenneville, J.; Martinez, T. J.; Wolynes, P. G. *J. Phys. Chem. A* **2003**, *107*, 10706–10716.
- (5) Dou, Y.; Allen, R. E. *J. Chem. Phys.* **2003**, *119*, 10658–10666.
- (6) Waldeck, D. H. *Chem. Rev.* **1991**, *91*, 415–436.
- (7) Choi, B. Y.; Kahng, S. J.; Kim, S.; Kim, H.; Kim, H. W.; Song, Y. J.; Ihm, J.; Kuk, Y. *Phys. Rev. Lett.* **2006**, *96*, 156106–1–156106–4.
- (8) Gutiérrez, R.; Grossmann, F.; Schmidt, R. *ChemPhysChem* **2003**, *4*, 1252–1256.
- (9) Paci, B.; Schmidt, C.; Fiorini, C.; Nunzi, J. M.; Arbez-Gindre, C.; Screttas, C. G. *J. Chem. Phys.* **1999**, *111*, 7486–7492.

- (10) Papper, V.; Likhtenshein, G. I. *J. Photochem. Photobiol., A* **2001**, *140*, 39–52.
- (11) Dugave Ch. *Cis–Trans Isomerization in Biochemistry*; Wiley: New York, 2006.
- (12) Liu, R. S. H.; Hammond, G. S. *Proc. Natl. Acad. Sci. U.S.A.* **2000**, *97*, 11153–11158.
- (13) Fuß, W.; Kosmidis, C.; Schmid, W. E.; Trushin, S. A. *Angew. Chem., Int. Ed.* **2004**, *43*, 4178–4182.
- (14) Su, C.; Lee, L.-X.; Chen, C.-F. *Synth. Met.* **2003**, *137*, 865–866.
- (15) Tsai, C.-S.; Su, C.; Wang, J.-K.; Lin, J.-C. *Langmuir* **2003**, *19*, 822–829.

field under the tip of a scanning tunneling microscope (STM).<sup>17,18</sup> However, when molecules are adsorbed on surfaces, *trans*-*cis* isomerization mechanisms are usually described by isomer conformations that mimic those known in the gas phase. Yet for self-assembled monolayers,<sup>15,28</sup> molecular islands,<sup>16,18</sup> or isolated species,<sup>17</sup> steric hindrance involving the surface atoms or the neighboring molecules is expected to have a strong influence on the isomerization reactions rates and pathways as they are known from the gas. One of the aims of this Article is to demonstrate that, on surfaces, the search for isomerization should not be limited to reactions similar to those observed in the gas or liquid phase. New molecular conformations that are unstable in the gas or liquid phases may be stabilized through weak surface interactions.<sup>29</sup> Such surface isomers may lead to unique conformations that can be used to induce further molecular reactions or exhibit new molecular properties.

Here, we show that the *trans*-*cis* isomerization is not the most significant molecular reaction of the *trans*-stilbene molecule after its physisorption on the silicon surface. Instead, other molecular surface isomerizations combined with diffusion occurs. The molecular surface-isomerization reactions of individual stilbene molecules adsorbed on a Si(100)-2×1 surface are studied by using a low temperature STM at 5 K. Surprisingly, the STM topographies show that, the stilbene molecules, all initially in the *trans* configuration, adsorb on the Si(100)-2×1 at 12 K, either in the *trans* conformation (TS), in the *cis* conformation (CS), or in two new conformations I<sub>1</sub> and I<sub>2</sub>. These isomerization reactions appear to spontaneously occur during the adsorption processes. Subsequently, we use the STM tip as a local source of tunnel electrons to electronically excite individual stilbene molecules on the surface with the aim to activate molecular surface-isomerization reactions. As a result, the molecule is observed to diffuse across the surface and to isomerize according to the TS → I<sub>1</sub> and CS → I<sub>2</sub> reactions, respectively. The reverse reactions (i.e., I<sub>1</sub> → TS and I<sub>2</sub> → CS) can be activated as well. Electronic excitation could not activate either the TS ↔ CS

isomerization as observed in the gas phase or the I<sub>1</sub> ↔ I<sub>2</sub> transformation. Moreover, the diffusion and isomerization quantum yields measured on n-type substrates show a considerable increase as compared to p-type doped silicon substrates.

## 2. Experimental Section

The experiments performed with an ultrahigh vacuum (UHV) low temperature Besoke type STM (LT-STM) cooled to 5 K, as well as the sample preparation, have been described previously.<sup>30</sup> The Si(100) samples used for this study are p-doped (B,  $\rho \approx 0.006 \Omega \text{ cm}$ ) and n-doped (As,  $\rho \approx 0.004 \Omega \text{ cm}$ ). After cleaning the surface, the manipulator clamping the sample holder is cooled to  $\sim 6 \text{ K}$ .<sup>30</sup> Under these experimental conditions, the silicon sample surface has an estimated temperature of 12 K.<sup>31</sup> The commercially available *trans*-stilbene powder used from Sigma-Aldrich has a purity of 96%. To introduce *trans*-stilbene molecules in the preparation chamber through a leak valve, we gently heat the solid *trans*-stilbene in its flask to  $\sim 370 \text{ K}$ . Under these conditions, we adsorb  $\sim 0.09$  monolayers of *trans*-stilbene molecules by exposing the Si(100) surface at 12 K to a pressure of  $2.2 \times 10^{-9}$  torr during 40 s. In this study, the low surface temperature is deliberately chosen to favor physisorption so that the stilbene molecules retain their native properties as much as possible. Indeed, room temperature surface adsorption on clean Si(100)-2×1 may induce the dissociative chemisorption of stilbene molecules due to the highly reactive dangling bonds on the silicon surface. After molecular adsorption, the silicon sample is transferred to the LT-STM chamber for analysis.

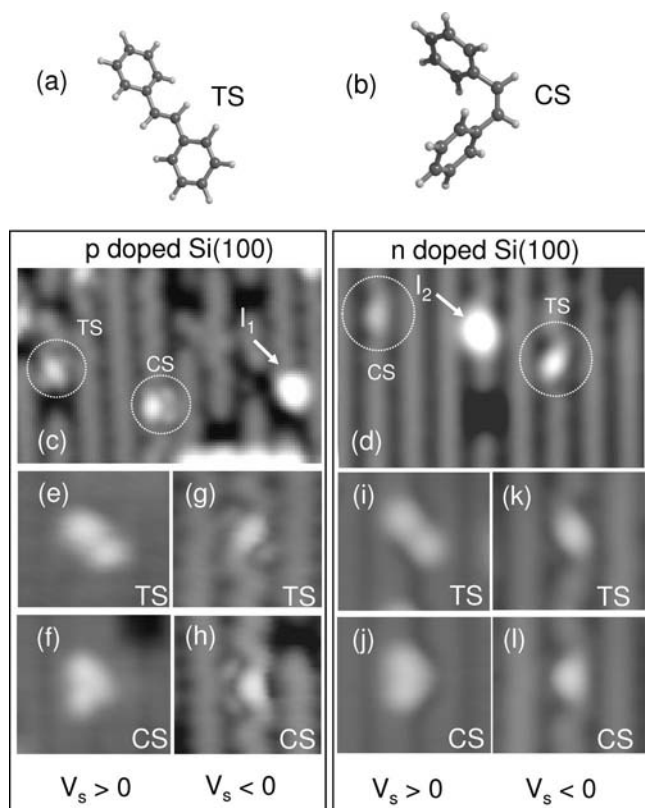
## 3. Stilbene Adsorption Conformations

Figure 1 shows STM topographies of various stilbene conformations observed on the Si(100)-2×1 surface, following the adsorption of the *trans*-stilbene molecules, on both p-doped and n-doped samples. Gas-phase molecular conformations of *trans*-stilbene (TS) and *cis*-stilbene (CS) are shown for comparison in Figure 1a and b. For each type of dopant (n or p), four different adsorption conformations of stilbene (TS, CS, I<sub>1</sub>, and I<sub>2</sub>) are observed (Figure 1c and d). From their shape and symmetry, the STM topographies shown in Figure 1e, g, i, k are assigned to the *trans*-stilbene (TS) isomer conformation, whereas the conformations observed in Figure 1f, h, j, and l are assigned to the *cis*-stilbene (CS). Indeed, the empty state topographies ( $V_s > 0$ ) of Figure 1e and i correlate well with the shape of the *trans*-stilbene in the gas phase shown in Figure 1a, whereas the empty state topographies ( $V_s > 0$ ) of the CS conformation (Figure 1f and j) match the shape of the *cis*-stilbene in the gas phase (see Figure 1b). The other observed isomers I<sub>1</sub> and I<sub>2</sub> (see arrows in Figure 1c and d) might be surface-isomer conformations and will be discussed later. The TS conformation in Figure 1e and i appears elongated and oriented at  $48^\circ$  with respect to the dimer rows, while the CS conformation in Figure 1f and j looks folded in a crescent shape. In these unoccupied state ( $V_s > 0$ ) STM topographies (Figure 1e, f, i, and j), the benzene rings appear as very bright spots in both the TS and the CS conformations. The occupied state STM topographies ( $V_s < 0$ ) show only slight differences when the type of dopant in the silicon changes. For p-doped silicon, the benzene rings of both the CS and the TS conformations (Figure

- (16) Tsai, C.-S.; Wang, J.-K.; Skodje, R. T.; Lin, J. C. *J. Am. Chem. Soc.* **2005**, *127*, 10788–10789.
- (17) (a) Henzl, J.; Mehlhorn, M.; Gawronski, H.; Rieder, K.-H.; Morgenstern, K. *Angew. Chem., Int. Ed.* **2006**, *45*, 603–606. (b) Henzl, J.; Bredow, Th.; Morgenstern, K. *Chem. Phys. Lett.* **2007**, *435*, 278–282.
- (18) Alemani, M.; Peters, M. V.; Hecht, S.; Rieder, K.-H.; Moresco, F.; Grill, L. *J. Am. Chem. Soc.* **2006**, *128*, 14446–14447.
- (19) Simic-Milosevic, V.; Mehlhorn, M.; Rieder, K.-H.; Meyer, J.; Morgenstern, K. *Phys. Rev. Lett.* **2007**, *98*, 116102-1–116102-4.
- (20) Liljeroth, P.; Repp, J.; Meyer, G. *Science* **2007**, *317*, 1203–1206.
- (21) Comstock, M. J.; Levy, N.; Kirakosian, A.; Cho, J.; Lauterwasser, F.; Harvey, J. H.; Strubbe, D. A.; Fréchet, J. M.; Trauner, D.; Louie, S. G.; Crommie, M. F. *Phys. Rev. Lett.* **2007**, *99*, 038301-1–038301-4.
- (22) Henningsen, N.; Franke, K. J.; Schulze, G.; Fernández-Torrente, I.; Priewisch, B.; Rück-Braun, K.; Pascual, J. I. *ChemPhysChem* **2008**, *9*, 71–73.
- (23) Fuchsels, G.; Klamroth, T.; Dokić, J.; Saalfrank, P. *J. Phys. Chem. B* **2006**, *110*, 16337–16345.
- (24) (a) Kudernac, T.; Jan van der Molen, S.; van Wees, B. J.; Feringa, B. L. *Chem. Commun.* **2006**, 3597–3599. (b) Bellec, A.; Cranney, M.; Chalopin, Y.; Mayne, A. J.; Comtet, G.; Dujardin, G. *J. Phys. Chem. C* **2007**, *111*, 14818–14822.
- (25) Hagen, S.; Leyssner, F.; Nandi, D.; Wolf, M.; Tegeder, P. *Chem-PhysChem* **2007**, *444*, 85–90.
- (26) Iancu, V.; Hla, S. W. *Proc. Natl. Acad. Sci. U.S.A.* **2006**, *103*, 13718–13721.
- (27) Jäckel, F.; Watson, M. D.; Müllen, K.; Rabe, J. P. *Phys. Rev. Lett.* **2004**, *92*, 188303-1–188303-4.
- (28) Miwa, J. A.; Weigelt, S.; Gersen, H.; Besenbacher, F.; Rosei, F.; Linderroth, T. R. *J. Am. Chem. Soc.* **2006**, *128*, 3164–3165.
- (29) Martin, M.; Lastapis, M.; Riedel, D.; Dujardin, G.; Mamatkulov, M.; Stauffer, L.; Sonnet, Ph. *Phys. Rev. Lett.* **2006**, *97*, 216103-1–216103-4.

- (30) Riedel, D.; Lastapis, M.; Martin, M.; Dujardin, G. *Phys. Rev. B* **2004**, *69*, 121301R-1–121301R-4.

- (31) The estimation of the temperature of the silicon sample surface is performed by a measurement made when a temperature probe (silicon diode) is fixed on a silicon sample during the helium cooling of the manipulator.



**Figure 1.** (a and b) Conformations of *trans*-stilbene (planar) and *cis*-stilbene in their gas-phase configuration, respectively. (c and d)  $69 \times 44 \text{ \AA}^2$  STM topographies of stilbene molecules adsorbed on p-doped and n-doped Si(100)- $2 \times 1$ , respectively. Circles indicate the *trans*-stilbene (TS) and *cis*-stilbene (CS) adsorption conformations. The arrows indicate stilbene surface isomers  $I_1$  and  $I_2$ , which are described in detail in Figure 3. (e, g, i, k)  $23 \times 23 \text{ \AA}^2$  STM topographies of the unoccupied ( $V_s = +1.5 \text{ V}$ ,  $I = 69 \text{ pA}$ ) and occupied ( $V_s = -1.5 \text{ V}$ ,  $I = 69 \text{ pA}$ ) *trans*-stilbene conformations on a p-doped (e and g) and n-doped (i and k) silicon surface. (f, h, j, l)  $23 \times 23 \text{ \AA}^2$  STM topographies of the unoccupied ( $V_s = +1.5 \text{ V}$ ,  $I = 69 \text{ pA}$ ) and occupied ( $V_s = -1.5 \text{ V}$ ,  $I = 69 \text{ pA}$ ) *cis*-stilbene on a p-doped (f and h) and n-doped (j and l) silicon surface.

1g and h) appear brighter than for n-doped silicon (Figure 1k and l), while the unoccupied states look almost the same. This difference between p-doped and n-doped samples and the shapes of the various observed conformations under STM has been observed routinely with more than four different tips and samples.

As explained in the Experimental Section, before adsorption, the stilbene molecules were initially in the *trans* conformation (TS). After adsorption, the observed proportions of the TS, CS,  $I_1$ , and  $I_2$  conformations in the STM topographies are 14%, 17%, 17%, and 28%, respectively (the remaining 24% of the adsorbed species are classified as unknown species). To rule out the possibility of isomerization of the initial TS conformation during the heating of the stilbene flask, nuclear magnetic resonance (NMR) spectroscopy of the molecules, in the flask, was performed before and after the experiment. The flask was screened to prevent ambient light pollution. No change was noticed, indicating that the isomerization observed in the STM topographies occurs during the adsorption of the molecule on the Si(100) surface. Furthermore, the proportion of the various stilbene conformations observed after adsorption does not appreciably change as a result of heating the solid stilbene over a range of temperature (from 370 to 403 K) used to heat the

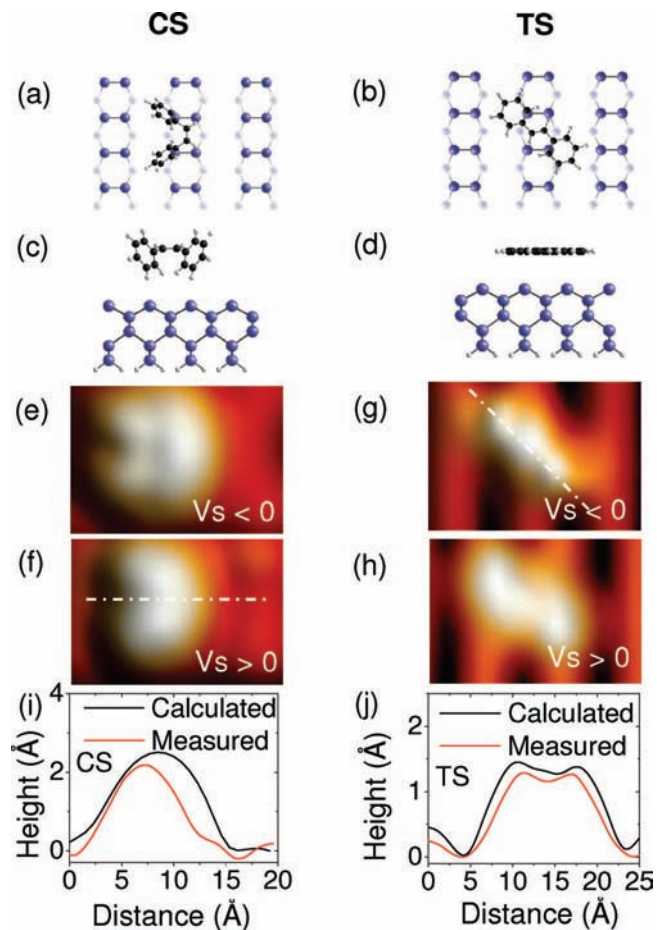


**Figure 2.** Top views (a and b) and side views (c and d) of the conformation of the *cis*-stilbene and *trans*-stilbene molecules relative to the Si(100)- $2 \times 1$  surface used for STM topography simulations. (e and f) Occupied ( $V_s = -1.2 \text{ V}$ ) and unoccupied ( $V_s = +1.5 \text{ V}$ ) calculated STM topographies of the *cis*-stilbene, respectively. (g and h) Occupied ( $V_s = -1.2 \text{ V}$ ) and unoccupied ( $V_s = +1.5 \text{ V}$ ) calculated STM topographies of the *trans*-stilbene molecule, respectively. The STM topographies were calculated at a constant current of 70 pA. (i and j) Comparison of the measured and calculated profiles (see the dashed lines on (f) and (g)) on a CS and a TS molecule, respectively.

solid stilbene. This confirms that the *trans*–*cis* isomerization does not occur during evaporation.

The Si(100)- $2 \times 1$  surface has been shown to be very reactive toward molecules with C–C double bonds due to the presence of the silicon dimer  $\pi$  orbitals.<sup>32</sup> One might expect stilbene molecules to react similarly. However, from the STM topographies in Figure 1, there are strong indications that physisorption occurs rather than chemisorption of the stilbene molecules on the Si(100)- $2 \times 1$  surface at 12 K. For both *cis* and *trans* isomers, the bright protrusion observed in the occupied state STM topographies, which corresponds to the position of the carbon double bond of the stilbene molecule, is always observed to be centered on the dimer row and in a position between two silicon dimers (see Figure 2a–d for the proposed adsorption conformation and Figure 1g and h for the dimer positions). If chemisorption occurred during the adsorption at 12 K, this would involve the breaking of the carbon double bond followed by bond formation with the silicon dimers similar to reactions

(32) Clemen, L.; Wallace, R. M.; Taylor, P. A.; Dresser, M. J.; Choyke, W. J.; Weinberg, W. H.; Yates, J. T. *Surf. Sci.* **1992**, *268*, 205–216.

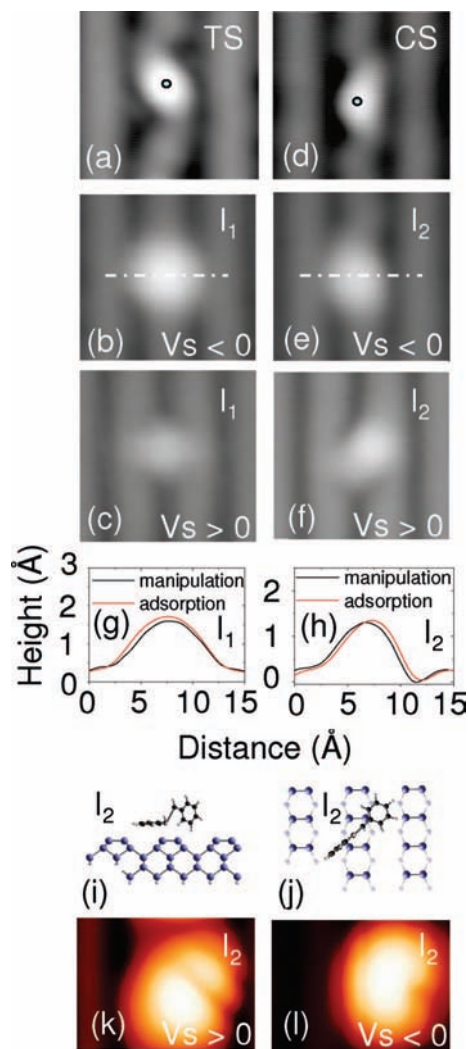


**Figure 3.**  $19.2 \times 18 \text{ \AA}^2$  STM topographies of stilbene molecules adsorbed on an n-doped Si(100)- $2 \times 1$  surface. (a and d) Occupied state ( $V_s = -1.5 \text{ V}$ ,  $I = 69 \text{ pA}$ ) of the *trans*-stilbene and *cis*-stilbene molecules before a manipulation (the excitation is applied on the circle at  $V_s = -2.5 \text{ V}$ ,  $I = 780 \text{ pA}$ , for a duration of 3.2 s). (b and e) Occupied state ( $V_s = -1.5 \text{ V}$ ,  $I = 69 \text{ pA}$ ) STM topographies of the surface-isomer  $I_1$  of the *trans*-stilbene molecule after the manipulation in (a) and the surface-isomer  $I_2$  of the *cis*-stilbene molecule after the manipulation in (d), respectively. (c and f) Same image as (b) and (e) in the unoccupied state ( $V_s = +1.5 \text{ V}$ ,  $I = 69 \text{ pA}$ ). (g and h) Profiles measured on  $I_1$  and  $I_2$  surface-isomers STM topographies, respectively (see dotted lines in (b) and (e)), before adsorption and after manipulation. (i) Top and (j) side views of a suggested conformation of the  $I_2$  surface isomer. (k and l) Calculated STM topographies of the proposed  $I_2$  surface isomer for, respectively, the unoccupied state ( $V_s = +1.5 \text{ V}$ ) and occupied state ( $V_s = -1.5 \text{ V}$ ) at  $I = 70 \text{ pA}$ .

described in ref 33. In this case, the corresponding STM topographies of the molecules, especially the CS conformation, would be expected to be rotated by  $90^\circ$  as compared to what is observed in Figure 2a. Indeed, it is unlikely that chemisorption occurs with a C–C double bond direction of the CS molecules perpendicular to the silicon dimer direction.<sup>33</sup> Furthermore, the physisorbed character is consistent with recent results obtained by synchrotron radiation photoemission in which only a weak

$\pi$ – $\pi$  bonding between the stilbene and the Si(100) surface was observed at low coverage on Si(100)- $2 \times 1$  at 100 K.<sup>34</sup>

#### 4. Theoretical Methods

To verify the proposed adsorption conformations in Figure 2a and b, we have calculated the STM topographies of both CS and TS molecules physisorbed on the Si(100)- $2 \times 1$  surface. It is known that ab initio Density Functional Theory (DFT) methods, for example in the Local Density Approximation (LDA), poorly describe weak interactions such as van der Waals (VdW) forces. Therefore, adsorption energy calculations of the CS and TS molecules on the Si(100) surface obtained with this method would not be relevant. Although some very recent methods based on VdW-DFT calculations are intended to describe more accurately weakly bonded adsorbates, it is very difficult to build an appropriate VdW functional adapted to physisorbed stilbene molecules on a reconstructed silicon surface.<sup>35,36</sup> Furthermore, such a method will probably involve a heavy computational cost.

Here, we propose an alternative approach that consists of identifying adsorption conformations on the basis of successive comparisons of calculated and experimental STM images. For these calculations, we use a tight binding scheme that correctly reproduces first-principles based density functional electronic structure calculations with a low computational cost. This allows complex systems to be handled with adequate sensitivity as compared to classical DFT methods.<sup>36–38</sup> To simulate the Si(100) surface, we consider a single slab of 5 planes, each of which contains 24 silicon atoms. The lower plane is passivated by hydrogen atoms. The upper one is reconstructed to form the surface dimers. In the directions parallel to the surface, the system including the Si slab and the molecules is periodic and is built from a supercell corresponding to 12 ( $3 \times 4$ ) dimers. This supercell is large enough to avoid interactions between adsorbed molecules and thus provides a good simulation of STM images. For the same reason, the electronic structure of the interacting system (molecule and surface) is calculated only at  $\vec{k} = \vec{0}$ , using the self-consistent density functional-based tight binding method developed in the DFTB+ code.<sup>39</sup> Within this approach, the parametrization of the Hamiltonian has been validated on various molecular systems, including weakly interacting ones.<sup>40</sup> The tunneling current is then calculated between the STM tip, which is assumed to have a pyramidal apex, and the sample. The elastic scattering approach considers that electrons tunneling occurs through multiple channels, although the electron transport through the STM junction is treated in the coherent regime. It is also possible to include tip effects while the tip geometry has only a weak influence on the

(33) (a) Carbone, M.; Palma, A.; Caminiti, R. *Phys. Rev. B* **2007**, *75*, 245332-1–245332-8. (b) Zhu, J.; Pan Wang, Y. X.; Wei, Q.; Zang, L. K.; Zhou, L.; Liu, T. J.; Jiang, X. M. *Appl. Surf. Sci.* **2007**, *253*, 4586–4592.

(34) Schmidt, P. M.; Horn, K.; Dil, J. H.; Kampen, Th. U. *Surf. Sci.* **2007**, *601*, 1775–1780.  
 (35) Rydberg, H.; Lundqvist, B. I.; Langreth, D. C.; Dion, M. *Phys. Rev. B* **2000**, *62*, 6997–7006.  
 (36) Hooper, J.; Cooper, V. R.; Thonhauser, T.; Romero, N. A.; Zerilli, F.; Langreth, D. C. *ChemPhysChem* **2008**, *9*, 891–895.  
 (37) Dubois, M.; Delerue, C.; Allan, G. *Phys. Rev. B* **2005**, *71*, 165435-1–165435-6.  
 (38) Dubois, M.; Delerue, C.; Rubio, A. *Phys. Rev. B* **2007**, *75*, 041302(R)-1041302(R)-4.  
 (39) Elstner, M.; Porezag, D.; Jungnickel, G.; Elsner, J.; Haugk, M.; Frauenheim, Th.; Suhai, S.; Seifert, G. *Phys. Rev. B* **1998**, *58*, 7260–7268.  
 (40) Krüger, T.; Elstner, M.; Schiffels, P.; Frauenheim, T. *J. Chem. Phys.* **2005**, *122*, 114110-1–114110-6.

results.<sup>41</sup> More complex methods based on the nonequilibrium Green's functions formalism (also known as the Keldysh approach) are not necessary in the present case, because interactions between the tip and the sample remain weak due to the low tunneling current during image acquisition.

The initial conformations of the CS and TS molecules are calculated by energy minimization in the gas phase, while the silicon surface is minimized independently. After separate minimizations in the gas phase, the corresponding molecular conformations of the CS and the TS molecules were tested, on the silicon surface (see Figure 2a–d), by small variations of different parameters such as: (i) slight rotations on one or both benzene rings with respect to the benzene–ethene bond axis, (ii) change of the molecule to surface distance, (iii) rotation of the whole molecule with respect to the dimer row direction and translation of the molecule along the dimer rows, and (iv) change of the buckling of the silicon dimers surface. Any of these factors can dramatically modify the result of the calculated image. Numerous adsorption geometries were tested, taking into consideration a variety of rotations and translations of the whole molecule with respect to the dimer row direction. We emphasize that none of the tested conformations matches the I<sub>1</sub> or I<sub>2</sub> STM topographies. This result indicates that the observed stilbene conformations I<sub>1</sub> and I<sub>2</sub> are not simply a change between two different adsorption orientations of the TS or CS conformations.

The calculated STM images of the CS and TS conformations that best match the experimental ones are shown in Figure 2. The average molecule–surface distance is 4.2 and 3.2 Å in Figure 2c and d for the CS and the TS molecules, respectively. For both the CS and the TS molecules, there is a reasonably good agreement between the calculated (Figure 2) and the experimental (Figure 1) STM topographies for occupied and unoccupied states (see Figure 1e–l) acquired in constant current mode. The observed angle of the CS molecules in the experimental STM topographies can vary (mainly due to silicon dimer buckling) and is estimated to be  $71 \pm 13^\circ$ . The influence of the silicon dimer buckling is difficult to reproduce in our STM topography calculations. Thus, the apparent angle between the two benzene rings of the calculated CS STM topography of  $\sim 60 \pm 3^\circ$  (Figure 2e) is in sensible agreement with the observed experimental angles.

Our model reproduces relatively well the variation of the tunnel current with the variations of the tip–surface distance.<sup>42</sup> Therefore, the profiles obtained from the STM topographies of the measured and calculated CS and TS molecules can be compared as shown in Figure 2i and j. Both profiles show very similar tip heights above the stilbene molecules. These calculations support the choice of the orientations of the CS and TS molecules described in Figure 2a–d. Furthermore, the average height of these molecules relative to the silicon surface is too large for chemical bond formation, indicating that they are physisorbed on this surface. However, it should be noted that the calculated STM images of the TS molecules exhibit less contrasted contours than do the experimental ones (see Figure 1g and h). This is most probably due to the influence of the silicon surface interaction with the stilbene molecule, which changes with the type of dopant (n or p). Indeed, it has been shown that the strongly doped samples used for low temperature

STM experiments can influence STM topographies.<sup>43</sup> Unfortunately, this influence cannot be taken into account in our calculations.

## 5. STM Manipulations of Stilbene Molecules

The STM topographies of both trans (TS) and cis (CS) isomers of stilbene molecules adsorbed on Si(100) have been identified in parts 3 and 4. Here, we use STM manipulation of single stilbene molecules to try to identify the nature of the observed I<sub>1</sub> and I<sub>2</sub> stilbene surface isomers. This is performed by reversibly changing the molecular conformation of *trans*-stilbene (TS) or *cis*-stilbene (CS) and vice versa. For that purpose, we use the following procedure: (i) after imaging a single molecule, the STM tip is positioned on top of a given part of the molecule, (ii) the feedback loop is switched off, and a negative surface voltage  $V_s$  is applied for a certain time (from 20 ms to 10 s), and (iii) the tip-to-surface distance is adjusted to obtain a given tunnel current  $I$ . The succession of these three steps is called a manipulation. During this procedure, the tunnel current is recorded as a function of time. Any abrupt change of the tunnel current at time  $t_{\text{exc}}$ , after the beginning of a manipulation, indicates that the molecule has diffused away from the STM tip position with or without a change in the molecular conformation. The resulting molecular conformation and position are determined by afterward STM imaging. The manipulation is repeated several times on the same molecule to obtain the statistical distribution of the quantity of charge  $Q = I \cdot t_{\text{exc}}$ . From this, we can deduce the quantum yield per electron  $Y = eI \cdot t_{\text{exc}}$  of the molecular reactions.<sup>44</sup> A surface voltage of  $-2.5$  V is chosen to remove electrons from the highest occupied molecular orbitals (HOMO) of the stilbene molecule. Indeed, as physisorbed species, the adsorbed stilbene molecules are expected to have a HOMO at about 2.2 eV and a HOMO–2 at 3.4 eV below the Fermi level.<sup>34</sup> Therefore, the manipulation is triggered by an electronic excitation, which consists of the formation of a positively charged stilbene molecule.<sup>44</sup> In the following, we will concentrate on the analysis of the various changes of molecular conformations that can be achieved by STM manipulation. We will also investigate the role of the type of dopant (n or p) in silicon on the dynamics of the various molecular processes.

**5.1. Diffusion and Isomerization of Stilbene Molecules.** Electronic excitation of a stilbene molecule in its TS conformation (the position of the tip is indicated by the dot in Figure 2a) results in the diffusion of the molecule across the surface. After diffusion, the molecule can be found either in the same TS conformation or in a new surface-isomer conformation called I<sub>1</sub> (Figure 3b and c). Similarly, the electronic excitation of a stilbene molecule in its CS conformation (Figure 3d) results in its diffusion across the surface. Most of the time, the diffusion of the CS molecule is accompanied by a change of molecular conformation into another surface-isomer conformation called I<sub>2</sub> (Figure 3e and f). These two new molecular conformations I<sub>1</sub> and I<sub>2</sub> show very similar spherical shapes in the occupied state STM topographies (Figure 3b and e). However, clear differences are visible in the unoccupied state STM topographies (Figure 3c and f). In fact, the bright spot in Figure 3b (conformation I<sub>1</sub>) is observed in the middle of the silicon dimer

(41) Perdigão, L.; Deresmes, D.; Grandidier, B.; Dubois, M.; Delerue, C.; Allan, G.; Stiévenard, D. *Phys. Rev. Lett.* **2004**, *92*, 216101-1.

(42) Lefebvre, I.; Lannoo, M.; Allan, G.; Martinage, L. *Phys. Rev. B* **1988**, *88*, 8593–8601.

(43) Lastapis, M.; Martin, M.; Riedel, D.; Dujardin, G. *Phys. Rev. B* **2008**, *77*, 125316-1–125316-6.

(44) (a) Lastapis, M.; Martin, M.; Riedel, D.; Hellner, L.; Comtet, G.; Dujardin, G. *Science* **2005**, *308*, 1000–1003. (b) Mayne, A. J.; Riedel, D.; Comtet, G.; Dujardin, G. *Prog. Surf. Sci.* **2006**, *81*, 1–51.

row, while a careful observation of the bright spot in Figure 3e (conformation  $I_2$ ) shows that it is slightly misaligned with the silicon dimer rows (gray vertical lines). Moreover, Figure 3g and h depicts the comparison between the profiles of both surface-isomers  $I_1$  and  $I_2$  after adsorption and after manipulation, respectively. These profiles are very similar, indicating that the surface isomers produced after adsorption and by manipulation are the same.

The molecular conformation changes induced by STM manipulation,  $TS \rightarrow I_1$  or  $CS \rightarrow I_2$ , are found to be reversible. Indeed, as shown in the series of images in Figure 4, when an electronic excitation is applied to an  $I_1$  molecule (shown by the small circles), the  $I_1 \rightarrow TS$  molecular conformation change can be observed (see Figure 4c and d). Although not shown, for clarity, in the series in Figure 4e–h, the occasional  $I_2 \rightarrow CS$  reaction can be also activated by similar STM manipulations. The  $I_1$  and  $I_2$  surface isomers are unequivocally associated with their initial molecular conformations (i.e., TS and CS, respectively). Indeed, the  $TS \leftrightarrow I_2$  or  $CS \leftrightarrow I_1$  conformation changes are never observed. Moreover, despite performing several hundred STM manipulations, neither the  $I_1 \leftrightarrow I_2$  nor the  $TS \leftrightarrow CS$  reactions are observed after manipulation with surface voltage up to  $V_s = -4$  V.

In light of these results, we can discuss the formation of the various stilbene conformations despite evaporating only TS molecules on the silicon surface. After deposition of the TS molecule at 12 K, the observation on the silicon surface of the TS, CS,  $I_1$ , and  $I_2$  conformations at 5 K suggests that specific adsorption processes occur since the  $TS \leftrightarrow CS$  isomerization could not be activated by the STM manipulations. The  $TS \rightarrow CS$  isomerization, which is observed to occur only during the adsorption process, can be considered as a low energy process as compared to STM manipulations because it involves only the thermal energy of the landing molecules. However, during the adsorption, a stilbene molecule from the gas phase can experience many possible conformations relative to the surface, thus exploring a large region of the reaction potential energy surface. Once the molecule is adsorbed, this potential energy surface is modified, leading to different reaction pathways.

The proportions of the TS, CS, and  $I_1$  conformers observed after adsorption are very similar ( $\sim 16\%$ ), yet they are significantly lower than the proportion of the  $I_2$  conformer ( $\sim 28\%$ ). While the CS and  $I_1$  conformers can be formed, with the same efficiency, via the  $TS \rightarrow CS$  or  $TS \rightarrow I_1$  reactions only during adsorption, the higher proportion of the  $I_2$  conformer might be explained by the existence of two reactional pathways. The first one corresponds to the direct  $TS \rightarrow I_2$  process, which can be activated during the adsorption, similar to the  $TS \rightarrow CS$  reaction. If we assume that the efficiency of the  $TS \rightarrow I_2$  process is similar to the  $TS \rightarrow CS$  and  $TS \rightarrow I_1$  ones (0.16), the second formation pathway can be obtained through the intrinsic precursor-mediated adsorption of the CS conformer, following the formation of the CS conformer via the  $TS \rightarrow CS$  process (see Figure 4i). Indeed, we will see in the following that the  $CS \rightarrow I_2$  isomerization is favored once the CS conformer is formed on the silicon surface. This proposed adsorption reactional scheme reveals principally that the surface is the main actor behind the formation of these particular surface isomers rather than any specificity of the STM excitation process itself.

The two molecular conformations  $I_1$  and  $I_2$  are inherent to the TS and CS molecules, respectively. We emphasize here that the observation of these surface isomers is related to the existence of single stilbene conformers, formed and stabilized

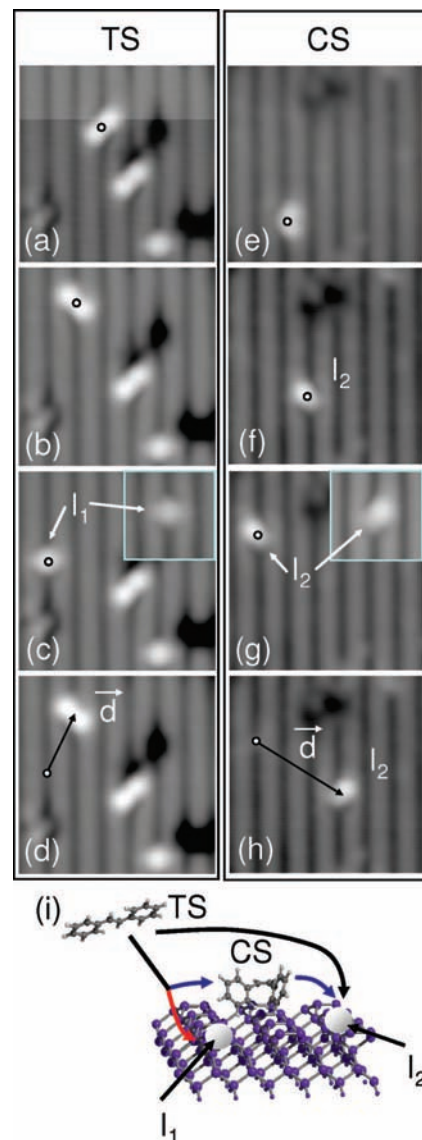


**Figure 4.** A series of  $54 \times 54 \text{ \AA}^2$  unoccupied state STM topographies illustrating the manipulation of stilbene molecules after an electronic excitation ( $V_s = -2.5$  V,  $I = 550$  pA, duration of 3.2 s) on an n-doped Si(100)- $2 \times 1$  surface. (a)–(d) and (e)–(h) are two separate series of manipulations starting from a TS and a CS conformation, respectively. A manipulation is applied, after each topography, with the STM tip located at the dot position. The (a)–(d) series STM topographies show a sequence of  $TS \rightarrow TS$  diffusion,  $TS \rightarrow I_1$  molecular surface isomerization with a diffusion, and the reverse manipulation  $I_1 \rightarrow TS$  with a diffusion, respectively. The series of STM topographies (e)–(h) show a sequence of  $CS \rightarrow I_2$  molecular surface isomerization combined with diffusion with a diffusion, followed by three diffusions of the  $I_2$  surface-isomer. The diffusion vector  $\vec{d}$  is defined as shown in (d) and (h). The insets in (c) and (g) are copies of Figure 3c and f for comparison. (i) Proposed adsorption scheme for the process of the TS molecule landing on the silicon surface during the initial formation of the various conformers CS,  $I_1$ , and  $I_2$ .

by the presence of the silicon surface, which might not be observed in the gas phase. These single molecule conformers are different from other observations made in self-assembled monolayer<sup>15,28</sup> or molecular islands.<sup>16,18</sup> In these cases, although the observed isomers conformations are probably perturbed by the substrate and the neighboring molecules, they are described as conformations resembling the *trans*–*cis* isomerization as depicted in the gas phase.

The STM topographies of the  $I_1$  and  $I_2$  surface isomers are very similar to each other but are extremely different from the

initial TS and CS conformations as observed in part 4. Indeed, none of the conformations tested during our STM image calculations showed any similarity to the  $I_1$  or  $I_2$  surface-isomer STM topographies. Our manipulations show a clear correlation between the TS- $I_1$  and CS- $I_2$  conformations; it is thus reasonable to suggest that the  $I_1$  and  $I_2$  surface isomers are similar to transient state conformations of the TS and CS molecules stabilized by the silicon surface.<sup>29,45,46</sup> From a theoretical point of view, the identification of the  $I_1$  and  $I_2$  conformations is a prohibitively heavy task as the comparison between experimental and calculated STM topographies will require many different configurations to be tested. Furthermore, a precise description of these molecular conformations will probably need to take into account the influence of the surface dopant type (n or p), which is difficult to implement in the calculations. As an example, STM topographies of a possible stilbene conformation analogous to transient state<sup>45,46</sup> are presented in Figure 3i–l and show clear similarities to the  $I_2$  surface isomer. This stilbene surface isomer is seen to have a different conformation as compared to the CS or TS molecules (Figure 3i and j). Here, the two benzene rings of the stilbene surface isomer are rotated by 90° from each other. Considering our theoretical approach, a more detailed description of the observed surface-isomers conformations is beyond the scope of this Article.

To understand the influence of the Si(100)-2×1 surface structure on the molecular diffusion induced by STM manipulation, we have performed a statistical analysis of the diffusion length and direction. As shown in Figure 4d and h, each manipulation is associated with a diffusion vector  $\vec{d}$  of the center of the molecule. The distribution of the diffusion distances in terms of coordinates  $d_x$  and  $d_y$  is shown in Figure 5. This shows the result of more than 150 manipulations at  $V_s = -2.5$  V with the molecules initially in the TS conformation and considering both final states TS and  $I_1$  (similar results are achieved for the molecules initially in the CS conformation). As we can see in these graphs (Figure 5), the molecules diffuse mainly to specific positions, periodically distributed along the  $x$  and  $y$  axis. In the background of the graph in Figure 5a, a STM topography (occupied states) of the clean Si(100)-2×1 surface is superimposed at the same scale with a grid to indicate the silicon dimer positions. As shown in Figure 5b and c, the distribution of events has a periodicity of  $7.6 \pm 0.1$  and  $4.1 \pm 0.2$  Å along the  $x$  and  $y$  axis, respectively. These periodicities are directly related to the Si(100)-2×1 structure where silicon dimers are separated by 7.7 Å between dimer rows and 3.85 Å along dimer rows.<sup>29</sup> A careful examination of Figure 5a shows that, for a constant diffusion distance, the stilbene diffusion occurs in almost the same proportion in all directions. However, chemisorbed species are known to diffuse anisotropically on the Si(100)-2×1 surface.<sup>47,48</sup> Therefore, the observed isotropic diffusion of the adsorbed stilbene molecules underlines their physisorbed character on the Si(100)-2×1 surface.

In this study, the molecular reaction induced by STM manipulation is always limited to the molecule underneath the STM tip, even when other molecules are located nearby (see, for example, Figure 4a–d). This indicates that the manipulation

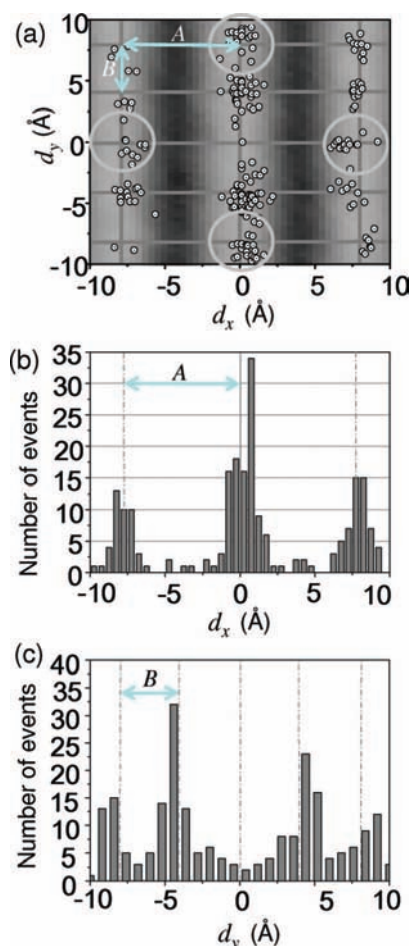


**Figure 5.** (a) Distribution of the diffusion vector coordinates  $d_x$  and  $d_y$  for the manipulation of *trans*-stilbene molecules ( $V_s = -2.5$  V,  $I = 1$  nA, for a duration of 3.2 s) on a p-doped Si(100)-2×1 surface. Both TS → TS and TS →  $I_1$  reactions are taken into account. A STM topography of the clean Si(100)-2×1 is superimposed at the same scale with an overlay grid indicating the silicon dimer positions. Light gray circles indicate final positions of the stilbene molecules, which have an equal diffusion distance  $\|\vec{d}\|$ . (b and c) Histograms of the  $d_x$  and  $d_y$  value, respectively. The  $A$  and  $B$  values indicate the distance between dimer rows and the distance between dimers along a dimer row, respectively.

process is most likely a local electron-induced process<sup>44</sup> rather than a nonlocal electrostatic field induced process.<sup>18</sup> For each type of molecular reaction induced by electronic excitation with the STM tip, we derive the corresponding quantum yield (probability of reaction per electron) by using the method described at the beginning of part 5. A typical example of a recorded current trace during a manipulation is shown in Figure 6c. The distribution of the binned number of electrons ( $t_{\text{exc}} \times I$ ) for the TS → TS and TS →  $I_1$  movements on a p-doped silicon sample is depicted in Figure 6a and b, respectively. To verify that these manipulations are induced by a single electron process, we have measured some reaction yields as a function of the tunnel current. Two examples of quantum yields are presented in Figure 6d for tunnel currents varying in the range  $10^{-10}$  to  $10^{-9}$  A. Both curves in Figure 6d show almost constant yields over this tunnel current range. This confirms that these molecular reactions are activated via a single tunnel electron process.<sup>49</sup>

The quantum yields as a function of the surface voltage for the four manipulations TS → TS, TS →  $I_1$ , CS → CS, and CS

(45) Han, G. W.; Lovell, T.; Liu, T.; Noodleman, L. *ChemPhysChem* **2002**, *3*, 167–178.

(46) Molina, V.; Merchán, M.; Roos, O. B. *J. Phys. Chem. A* **1997**, *101*, 3478–3487.

(47) Mo, Y. W. *Science* **1993**, *261*, 886–888.

(48) Wang, J. T.; Chen, C.; Wang, E. G.; Wang, D. S.; Mizuseki, H.; Kawazoe, Y. *Phys. Rev. Lett.* **2006**, *97*, 046103-1.

(49) (a) Stipe, B. C.; Rezaei, M. A.; Ho, W. *Science* **1998**, *279*, 1907–1909. (b) See also: Ho, W. *J. Chem. Phys.* **2002**, *117*, 11033–11061.

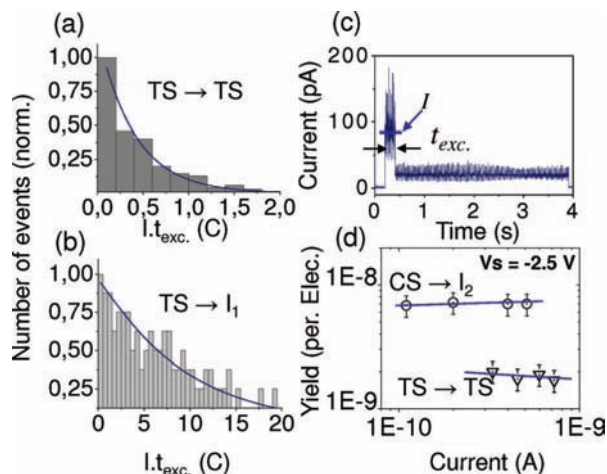


**Figure 6.** (a and b) Examples of the distribution of the amount of charge  $Q = I \cdot t_{\text{exc}}$  needed to manipulate a *trans*-stilbene molecule during a series of manipulations ( $V_s = -2.5$  V,  $I = 520$  pA, for a duration of 3.2 s) for the TS  $\rightarrow$  TS and the TS  $\rightarrow$  I<sub>1</sub> manipulations, respectively. The blue curves are exponential fits of the distributions. (c) A typical tunnel current trace recorded during the manipulation from which the average tunnel current  $I$  and the excitation  $t_{\text{exc}}$  are read. (d) Examples of the variation of the quantum yield as a function of the tunnel current for the CS  $\rightarrow$  I<sub>2</sub> (on an n-type silicon sample) and TS  $\rightarrow$  TS (on a p-type silicon sample) manipulations.

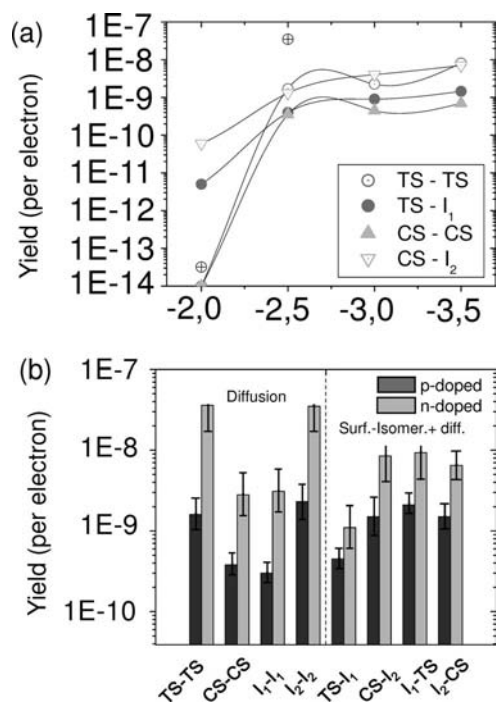


**Figure 7.** (a) Variation of the quantum yields as a function of the surface voltage for the TS  $\rightarrow$  TS, CS  $\rightarrow$  CS, TS  $\rightarrow$  I<sub>1</sub>, and CS  $\rightarrow$  I<sub>2</sub> reactions on a p-doped silicon sample. The curves that cross the symbols are to guide the eye. Note, for comparison, the two extra points indicating the quantum yields for the TS  $\rightarrow$  TS movement on an n-doped sample. (b) Comparison of the measured quantum yields of several observed manipulation processes involving diffusion only (TS  $\rightarrow$  TS, CS  $\rightarrow$  CS, I<sub>1</sub>  $\rightarrow$  I<sub>1</sub>, I<sub>2</sub>  $\rightarrow$  I<sub>2</sub>) or molecular surface isomerization combined with diffusion (TS  $\rightarrow$  I<sub>1</sub>, CS  $\rightarrow$  I<sub>2</sub>, I<sub>1</sub>  $\rightarrow$  TS, I<sub>2</sub>  $\rightarrow$  CS). Results are shown for p-type (dark gray) and n-type (light gray) doped silicon samples.

$\rightarrow$  I<sub>2</sub> on a p-type doped silicon sample are presented in Figure 7a. The four curves in Figure 7a show a similar behavior, that is, a strong increase of quantum yields when  $-2.5 < V_s < -2$  V and a plateau for  $V_s < -2.5$  V. This suggests that the four

observed molecular reactions are activated by the same type of electronic process. As mentioned before (beginning of part 5), this is expected to correspond to the removal of an electron from the HOMO orbitals of the stilbene molecule, resulting in a transient positive charging (oxidation) of the molecule, which is able to activate the various observed reactions. Therefore, in the following part of our study, we restricted the manipulations to  $V_s = -2.5$  V. This allows having quantum yields with similar order of magnitude either for a sole diffusion or for a diffusion combined with isomerization.

All of the quantum yields of the observed molecular reactions are shown in Figure 7b. From this graph, we note significant differences, especially for molecular reactions starting from the same initial conformation. For example, the yield  $Y_{\text{TS} \rightarrow \text{TS}}$  is much larger than  $Y_{\text{TS} \rightarrow \text{I}_1}$ , whereas  $Y_{\text{CS} \rightarrow \text{CS}}$  is considerably smaller than the yield  $Y_{\text{CS} \rightarrow \text{I}_2}$ . On the basis of the desorption induced by electronic transition (DIET) processes and considering that the electronic excitations are performed at a fixed voltage ( $V_s = -2.5$  V), it is believed that the electronic processes that induce the diffusion and the diffusion combined with an isomerization are expected to involve the same excited potential energy surface, for a given dopant, whatever the final conformation is. Therefore, the observed differences between the quantum yields for the various molecular reactions are attributed to specific molecular surface dynamics having different energy barriers of the molecular system in its electronic ground state. For physisorbed species, it seems reasonable a priori to consider that a simple molecular diffusion has a lower energy barrier than the molecular isomerization combined with diffusion. This is observed for the TS conformation because  $Y_{\text{TS} \rightarrow \text{TS}} > Y_{\text{TS} \rightarrow \text{I}_1}$ . Surprisingly, the opposite behavior is observed for the CS conformation because  $Y_{\text{CS} \rightarrow \text{CS}} < Y_{\text{CS} \rightarrow \text{I}_2}$ . In this latter case, one can anticipate that the energy barrier for diffusion of the CS conformation is higher than that for isomerization combined with diffusion in the I<sub>2</sub> conformation. From the ratios of the values reported in Figure 7b, we can plot a qualitative potential energy surface that describes the relative energy barriers, for a given dopant type, of the various observed molecular reactions following a manipulation. The two-dimensional qualitative potential energy surfaces shown in Figure 8 are formed from two asymmetric double potential wells. It shows several pathways for the manipulation performed on a TS molecule (Figure 8a) and a CS molecule (Figure 8b). The potential energy surface in Figure 8a illustrates how the electronic excitation of a TS molecule will induce diffusion rather than isomerization to I<sub>1</sub> ( $Y_{\text{TS} \rightarrow \text{TS}} > Y_{\text{TS} \rightarrow \text{I}_1}$ ). If a manipulation is applied to I<sub>1</sub>, the I<sub>1</sub>  $\rightarrow$  TS reaction will be favored rather than the diffusion of the I<sub>1</sub> surface isomer ( $Y_{\text{I}_1 \rightarrow \text{TS}} > Y_{\text{I}_1 \rightarrow \text{I}_1}$ ). In a different way, a manipulation on a CS molecule will induce isomerization to I<sub>2</sub> combined with diffusion rather than the CS  $\rightarrow$  CS diffusion (Figure 8b). Once in I<sub>2</sub>, the surface isomer has a lower barrier to overcome for diffusion than to induce the I<sub>2</sub>  $\rightarrow$  CS diffusion ( $Y_{\text{I}_2 \rightarrow \text{I}_2} > Y_{\text{I}_2 \rightarrow \text{CS}}$ ).

**5.2. The Role of the Type of Dopant in Silicon on the Molecular Surface-Isomerization Dynamics.** In the light of Figure 8, we can see that, in addition to having observed specific surface isomers of the stilbene molecule, the CS  $\leftrightarrow$  I<sub>2</sub> isomerization combined with diffusion and the TS  $\rightarrow$  TS diffusion are noticeably favored, as compared to the other reactions. A careful consideration of the quantum yields in Figure 7b shows that the molecular dynamics of these two processes are enhanced when the stilbene molecules are adsorbed on an n-doped silicon sample, although the relative barrier heights of the other



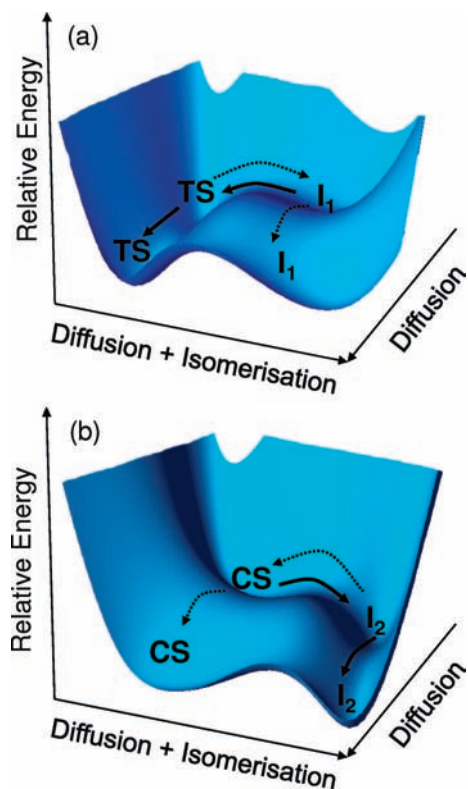


**Figure 8.** Qualitative potential energy surfaces illustrating the relative quantum yields for the various reaction pathways following electronic excitation induced by STM manipulations of (a) TS and  $I_1$  stilbene molecular conformations and (b) CS and  $I_2$  stilbene molecular conformations.

processes remain similar. To understand this phenomenon, we need to explore the role of the type of dopant on the dynamics of the various stilbene reactions induced by tunnel electrons excitation. The relative quantum yields ratios ( $Y_n/Y_p$ ) for n-doped and p-doped substrates are shown in Figure 9a. For all types of reactions, the yield is higher for n-doped than for p-doped silicon. Comparatively, surface diffusion is more influenced by the dopant type than the molecular surface isomerizations combined with diffusion.

The role of the type of dopant on molecular reactions on silicon surfaces has been rarely investigated. The influence of the type of dopant has been previously observed at the macroscopic scale in silicon etching,<sup>50</sup> during H atom photo-desorption processes from the Si(100)-2×1:H surface,<sup>51</sup> or in the adsorption of Li atoms on the Si(111):H surface.<sup>52</sup> Here, we investigate, at the level of a single molecule, the influence of the type of dopant on the molecular surface reactions induced by electronic excitation with the STM. Recent work has revealed the role of the type of dopant (n or p) in Si(100) on the surface dynamics of chemisorbed biphenyl molecules for which the quantum yields remain the same.<sup>43</sup> Here, it is the reaction yields that are modified by the type of doping (n or p) in silicon. This can be explained by the influence of surface charging when changing the type of dopant. With n-doped silicon, negative charging of surface states occurs, thus inducing upward band

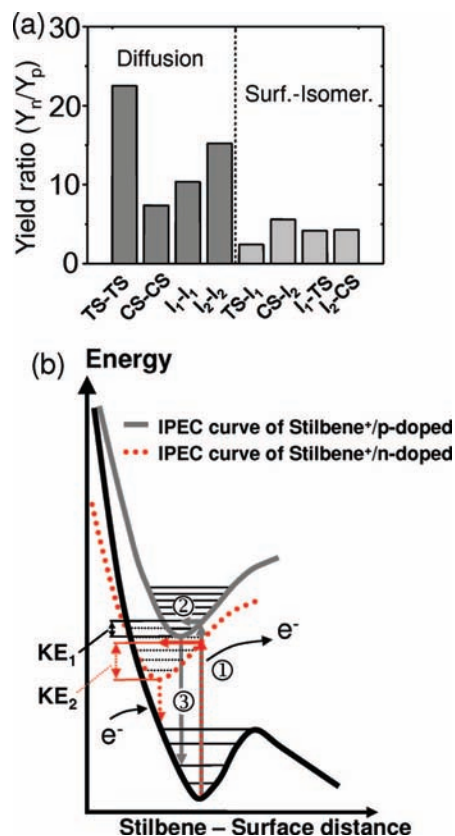


**Figure 9.** (a) Histogram of the relative quantum yield ( $Y_n/Y_p$ ) for the observed manipulation processes (TS  $\rightarrow$  TS, CS  $\rightarrow$  CS,  $I_1 \rightarrow I_1$ ,  $I_2 \rightarrow I_2$ , TS  $\rightarrow I_1$ , CS  $\rightarrow I_2$ ,  $I_1 \rightarrow$  TS,  $I_2 \rightarrow$  CS) between n-doped and p-doped silicon samples. (b) One-dimensional potential energy curves (PEC) and ionization potential energy curve (IPEC) of a stilbene molecule adsorbed on a silicon surface, illustrating the effect of the substrate type of dopant on the electronic excitation processes during a manipulation.

bending.<sup>53</sup> On p-doped silicon, the surface state charge is somehow more controversial but seems to remain neutral as observed by Liu et al.<sup>53</sup>

In the various STM topographies shown in Figure 1, there are no observable differences between the bright features (the C–C double bond of the stilbene molecule) where the electronic excitation is applied for the two dopant types (n or p). This further indicates that the type of dopant in the silicon weakly influences the electronic ground state of the stilbene molecule but principally plays a role in the electronic excited potential energy surface of the charged stilbene molecule. We have seen in paragraph 5.1 that the electronic excitation of the stilbene molecule proceeds via the formation of a transient molecular cation by removing one electron with the STM tip. When a stilbene molecule is adsorbed on a p-doped silicon surface, this process can be schematically represented by a one-dimensional potential energy curve (PEC) and an ionization potential energy curve (IPEC) in which the reaction coordinate is the molecule–surface distance (see transition ① between the black and gray curves in Figure 9b). Once the stilbene molecule is in its cationic form, its quantum states evolve on an ionized potential energy curve (light gray IPEC curve) by a rearrangement of its molecular structure (process ②). Next, it relaxes to the ground state, (i.e., via neutralization through an electron from the substrate) with an excess kinetic energy  $KE_1$  (transition ③). As a consequence

(50) Seidel, H.; Csepregi, L.; Heuberger, A.; Baumgärtel, H. *J. Electrochem. Soc.* **1990**, *137*, 3626–3632.

(51) Riedel, D.; Mayne, A. J.; Dujardin, G. *Phys. Rev. B* **2005**, *72*, 233304R-1–233304-4.

(52) Paggel, J. J.; Mannstadt, W.; Weindel, Ch.; Hasselblatt, M.; Horn, K.; Fick, D. *Phys. Rev. B* **2004**, *69*, 035310-1–035310-4.

(53) Liu, L.; Yu, J.; Lyding, J. W. *Mater. Res. Soc. Symp. Proc.* **2002**, *705*, Y6.6.1Y6.6.6.

of the ionization process, the stilbene molecule is attracted toward the surface by its image potential created in the silicon surface accordingly to the Antoniewicz model description.<sup>54</sup> The acquired vibrational energy in the ground state enables the barriers to be overcome for molecular diffusion or molecular surface isomerization.

When stilbene molecules are adsorbed on the n-doped Si(100)-2×1 surface, negative surface charges are believed to act on the physisorbed stilbene molecule by decreasing its ionization potential. A similar phenomenon has been recently depicted when a single carbon nanotube, closed by a fullerene cap, sees its ionization potential lowered by the presence of polar molecules such as water.<sup>55</sup> In the present work, the lowered ionization energy of the stilbene molecule, when adsorbed on n-doped silicon, can be described by a shift of the IPEC curve position toward lower energies. Additionally, the negatively charged surface should further increase the attraction of the stilbene molecule in its positively charged electronic excited states toward the surface. Therefore, the IPEC curve of the stilbene molecule adsorbed on n-doped silicon can be represented by the red dotted curve in Figure 9b. This new IPEC curve leads to a similar electronic excitation process ① to ③ resulting in an excess kinetic energy  $KE_2$  larger than  $KE_1$ , transferred in the electronic ground state, as shown in Figure 9b. The combination of these two phenomena, (i) the attractive energy potential curves toward the surface, and (ii) the reduced ionization potential of the stilbene molecule induced by the n-doped surface, is in good agreement with the large values of  $Y_n/Y_p$  reported in Figure 9a. It is also consistent with the absence of any significant energy shift in the curve of Figure 7a when compared to n-doped samples, because this combination of an attractive and lowered ionization potential energy curve leads to similar vertical ionization energies (process ① in Figure 9b).

From this model, it appears that, following tunnel excitation, the molecular surface dynamics related to the observed movement of a stilbene molecule occurs during the relaxation of its acquired vibrational energy in its ground state (Figures 8 and 9b). These molecular reactions are determined by the various energy barriers that the molecule has to overcome as described in Figure 8. Thus, a molecule adsorbed on an n-doped sample acquires additional kinetic energy in the ground state as compared to a p-doped surface. This energy is used for diffusion, as described in Figure 9b (i.e., partial desorption), and also allows more of the potential energy surface to be explored, leading to the observed molecular surface isomerization com-

bined with diffusion. Therefore, during these tunnel electron excitations, the control of the surface molecular dynamics seems to be mainly governed by the sole quantity of the corresponding acquired vibrational energy. However, it can be envisaged that various evolution of the molecular quantum states in the ionized potential energy curve (process ② in Figure 9b) can also slightly influence the starting point of the relaxation of the molecule in its ground-state potential energy surface. In this schematic point of view, a complete control of the tunnel electrons properties that induce STM electronic excitation would open up a way to optimize some reactional molecular pathways on single molecules. Stilbene molecules adsorbed on the Si(100)-2×1 surface can be good candidates for this type of study.

## 6. Conclusion

We have shown that *trans*-stilbene molecules adsorb on Si(100)-2×1 at 12 K in four different conformations: *trans*-stilbene (TS), *cis*-stilbene (CS), and two other surface-isomers conformations  $I_1$  and  $I_2$ . STM manipulation of individual stilbene molecules via electronic excitation has enabled us to study a number of reversible molecular surface reactions involving either only diffusion of the molecule across the surface (i.e.,  $TS \leftrightarrow TS$ ,  $CS \leftrightarrow CS$ ,  $I_1 \leftrightarrow I_1$ ,  $I_2 \leftrightarrow I_2$ ) or the diffusion combined with a change of molecular conformation ( $TS \leftrightarrow I_1$ ,  $CS \leftrightarrow I_2$ ). However, the *trans*-*cis* isomerization  $TS \leftrightarrow CS$ , which spontaneously occurs during the adsorption process, has not been observed during the STM manipulations. We have emphasized here that the concept of surface isomers is inherent to the observation of novel stable conformers on the silicon surface, which might not be observable in the gas phase or in matrices. These surface isomers open up a way to study new molecular properties on surfaces. Finally, the type of dopant (n or p) in silicon is shown to play an important role in the molecular dynamics through the measurement of the quantum yields of the observed stilbene surface reactions. These effects are ascribed to the negative charging of the n-doped silicon surface and are described by an Antoniewicz-like model.

**Acknowledgment.** This work is supported by the ANR N3M (contract no. ANR-05NANO-020-01), the European Integrated project PicoInside (contract no. FGP-015847), and the C'Nano programme of the region Ile de France. M.D. would like to thank Angel Rubio (Centro Mixto CSIC-UPV/EHU and Donostia International Physics Center) for helpful discussions. We also acknowledge the computer resources, technical expertise, and assistance provided by the Barcelona Supercomputing Center—Centro Nacional de Supercomputacion through the ETSF project.

JA807498V

(54) Antoniewicz, P. R. *Phys. Rev. B* **1980**, *21*, 3811–3814.

(55) Maiti, A.; Andzelm, J.; Tanpipat, N.; von Allmen, P. *Phys. Rev. Lett.* **2001**, *87*, 155502-1–155502-4.